ACS APPLIED MATERIALS & INTERFACES

Research Article

www.acsami.org

Silica Nanotubes Decorated by pH-Responsive Diblock Copolymers for Controlled Drug Release

Jiemei Zhou, Wenjian Zhang, Chunyan Hong,* and Caiyuan Pan

CAS Key Laboratory of Soft Matter Chemistry, Department of Polymer Science and Engineering, University of Science and Technology of China, Hefei, Anhui 230026, P. R. China

Supporting Information

ABSTRACT: A novel nanocontainer, which has silica nanotube (SNT) core and pH-sensitive polymer shell attaching on the exterior surface of silica nanotube, is presented in this paper. Polymer nanorods, which are conveniently fabricated though polymerization-induced self-assembly and reorganization method, are used as templates for the deposition of silica to fabricate hybrid nanorods. Calcination of as-synthesized silica hybrid nanorods leads to hollow SNTs. SNTs are functionalized with reversible addition−fragmentation chain transfer (RAFT) agent, then surface RAFT polymerization is conducted to get poly(2-(diethylamino)ethyl methacrylate)-*b*-poly(oligo(ethylene glycol) methacrylate)-coated SNTs (SNT-PDEAEMA-*b*-POEGMA). Doxorubicin (DOX) can be encapsulated in SNT-PDEAEMA-*b*-POEGMA, and controlled release of loaded DOX is achieved by adjusting pH of the medium. In vitro cell viability and cellular internalization study confirm the potential application of this nanocontainer in drug and gene delivery.

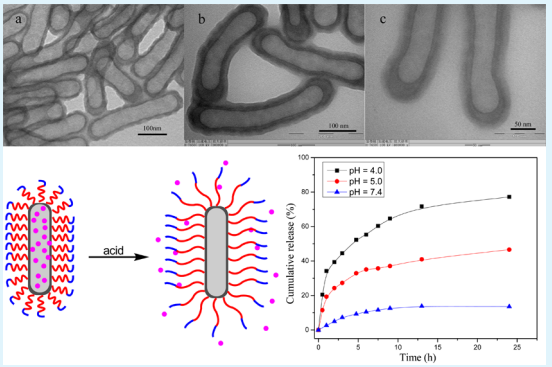

KEYWORDS: *silica nanotubes, controlled release, RAFT polymerization, nanocontainer*

1. INTRODUCTION

In recent years, controlled release systems for drugs and genes have received increased attention for the application in clinics. Various carrier materials including lipids, surfactants, polymer micelles, polymer gels, inorganic nanoparticles, and so on,[1−7] have been widely studied. Among these carrier materials, silica-based materials with well-defined structures are relatively nontoxic and biocompatible, these qualities are crucial for biomedical applications.[8−11] Various silica-based materials including silica nanowires, silica nanotubes (SNTs), mesoporous silica nanoparticles (MSNs), and hollow silica nanospheres,[12−14] have been fabricated. However, it is worth mentioning that most of silica-based materials used as drug vehicles for controlled release are silica spheres, especially MSNs,[15] which are usually decorated with smart caps responding to external stimuli[16−19] to regulate the drug release. Other shaped silica-based materials for drug delivery have been rarely studied to date. Huang et al.[20,21] reported the effects of particle shape on cellular uptake and circulation time in vivo, indicating that particles with larger aspect ratios have faster internalization rates and longer circulation times. The results indicate the promising application of nanoparticles with larger aspect ratios as carrier material for drug and gene delivery systems. Recently, silica nanotubes have attracted particular interest because of their anisotropic structure and high aspect ratio.[13] SNTs are considered as ideal nanocarriers of drugs due to their good biocompatibility and larger aspect ratios.

For the fabrication of SNTs, it is known that template-directed method, where the anisotropic templates determine the final nanostructures of SNTs, is a simple and straightforward route.[22−26] The applied templates are multiple, including cylindrical polymer brushes,[13,14,27,28] self-assembled nanowires,[29,30] multiwalled carbon nanotubes,[31] and peptides.[32] The preparation of these templates is either time-consuming and tedious or high-cost, which is difficult to scale up. For example, cylindrical polymer brushes were used as templates to fabricate SNTs with tunable dimensions.[13] However, the preparation of these polymer brushes was complicated and required multiple steps. The templates of self-assembly threadlike micelles of poly(ethylene glycol)-*block*-poly(4-vinylpyridine) have been used to fabricate SNTs.[31] The self-assembly approach is usually performed in dilute solution and is time-consuming, which hampers the expanded production of templates and the further applications of SNTs. It is imperative to develop a convenient method to synthesize SNTs with well-defined structure on a large scale for their applications. Our group has reported the preparation of nanomaterials by polymerization-induced self-assembly and re-organization (PISR) method recently,[33] which provides an easy way to prepare nanorods with controlled length and diameters.[34,35] The SNTs with different sizes have been fabricated using

Received: November 9, 2014
Accepted: January 27, 2015
Published: January 27, 2015

DOI: 10.1021/am507832n
ACS Appl. Mater. Interfaces 2015, 7, 3618−3625

polymer nanorods as templates.[36] However, SNTs have faint solubility in aqueous solution, and are not appropriate to be used as carrier directly. To improve the compatibility with biological systems and realize controlled release, SNTs should be modified further.

Herein, we attempt to construct a smart nanocarrier based on SNT for controlled release of drugs. Polymer nanorods with poly(2-(diethylamino)ethyl methacrylate) (PDMAEMA) corona and polystyrene (PS) core were prepared through PISR method. Using the polymer nanorods as templates, the silica/polymer hybrid nanorods were prepared. Subsequent calcination of these hybrid nanorods afforded the SNTs. This as-prepared material shows well-defined structure, and there are micropores that exist in the walls. SNTs were decorated by reversible addition-fragmentation chain transfer (RAFT) agent, and then diblock copolymers PDEAEMA-*b*-POEGMA (POEGMA = poly(oligo(ethylene glycol) methacrylate)) were grafted on the external surface of SNTs by RAFT polymerization. PDEAEMA is hydrophobic in neutral or alkaline solution, while in acidic solution it is hydrophilic. Taking advantage of the response of PDEAEMA to pH, SNT-PDEAEMA-*b*-POEGMA can realize the controlled release of drugs. Furthermore, POEGMA was selected to functionalize the SNTs to improve the dispersibility of SNTs in water, avoid agglomeration, and prolong blood circulation lifetime.[37,38] Doxorubicin (DOX) was encapsulated in SNT-PDEAEMA-*b*-POEGMA, and the controlled release of DOX from this nanocarrier can be achieved by adjusting pH of the medium. This nanocontainer showed low cytotoxicity and excellent endocytosis property. It is the first report to construct a controlled drug release system via decorating SNTs with pH-responsive diblock copolymer, to our knowledge. We expect that this novel silica/polymer hybrid nanotube could be applied in drug and gene delivery.

2. EXPERIMENTAL SECTION

2.1. Materials. The *S*-1-dodecyl-*S*′-(α,α′-dimethyl-α″-acetic acid) trithiocarbonate and 4-cyanopentanoic acid dithiobenzoate (CPDB) were synthesized as reported.[39,40] 2-Dimethylaminoethyl methacrylate (DMAEMA), 2-(diethylamino)ethyl methacrylate (DEAEMA), and oligo(ethylene glycol) methacrylate (OEGMA, M_n = 475 g/mol) were purchased from Aldrich and purified by passing through an alumina column to remove the inhibitor before polymerization. Styrene was purchased from Sinopharm Chemical Reagent Co. and distilled under reduced pressure prior to use. (3-Glycidyloxypropyl) trimethoxysilane (GLYMO) was purchased from Aldrich and distilled under reduced pressure prior to use. The 2,2′-azobis(isobutyronitrile) (AIBN) was purified by recrystallization from ethanol. Rhodamine B (RhB) and DOX were purchased from Aladdin and used as received. All other reagents of analytical grade were used as received.

2.2. Synthesis of Silica Nanotubes Using Polymer Nanorods as Templates. The polymer nanorods were synthesized by PISR method according to reference.[36] Into a 4 L flask, polymer nanorods (500 mg) dispersed in 1000 mL of methanol, 1000 mL of aqueous solution (pH = 4.0), and tetraethyl orthosilicate (TEOS, 25 g) were added in order. The mixture was stirred sufficiently at room temperature for 3 d, and the resultant solid was collected by centrifugation. The obtained hybrid silica nanorods were washed three times with ethanol and distilled water, respectively, and lyophilized. Subsequently, calcination of hybrid silica nanorods were conducted at 550 °C for 5 h to remove the polymer templates and other organic components to obtain the SNTs.

2.3. Synthesis of RAFT Agent Decorated Silica Nanotubes. SNTs (0.5 g) and GLYMO (2 mL, 8.57 mmol) were dispersed in dried toluene (14.3 mL), and the mixture was heated overnight at reflux under N_2 atmosphere. The glycidyl-functionalized SNTs were collected by filtration and washed extensively with dry toluene and methanol, respectively. After being dried overnight in a vacuum oven at room temperature, the resultant solids were suspended in methanol (45 mL). Hydrochloric acid (2.66 g) was added into the solution under stirring, and the mixture was heated at 70 °C for 24 h. The hydroxyl-functionalized SNTs (SNT−OH) were filtered, washed three times with methanol, and dried overnight in a vacuum oven at room temperature. Subsequently, SNT−OH (0.5 g), *S*-1-dodecyl-*S*′-(α,α′-dimethyl-α″-acetic acid) trithiocarbonate (3.64 g, 10 mmol), and 4-dimethylaminopryidine (DMAP, 1.528 g, 12.5 mmol) were added into dried dichloromethane (30 mL), and the mixture was stirred in the ice−water bath. Then *N*-ethyl-*N*′-(3-(dimethylamino)propyl)-carbodiimide hydrochloride (EDC·HCl, 2.936 g, 12.5 mmol) was added into the solution, and the esterification reaction was conducted at room temperature for 46 h. The mixture was centrifuged (10000 r/min, 15 min) and washed five times with distilled water, methanol, and acetone. The resulting SNT-RAFT was dried overnight in a vacuum oven at room temperature.

2.4. Synthesis of SNT-PDEAEMA-*b*-POEGMA. Typically, SNT-RAFT (50 mg), DEAEMA (1.85 g, 10 mmol), AIBN (2.0 mg, 0.012 mmol), and 5.0 mL of tetrahydrofuran (THF) were placed in a 10 mL polymerization tube. The solution was degassed by three freeze−pump−thaw cycles. After it was sealed, the polymerization tube was placed in oil bath at 70 °C for 21 h. The polymerization was stopped by cooling to room temperature. The mixture was centrifuged (10 000 rev/min, 15 min) and washed five times with THF. SNT-PDEAEMA was dried overnight in a vacuum oven at room temperature.

Subsequently, SNT-PDEAEMA (100 mg), OEGMA (0.95 g, 2 mmol), AIBN (0.4 mg, 0.0024 mmol), and 2.5 mL of THF were placed in a 5 mL polymerization tube. The solution was degassed by three freeze−pump−thaw cycles, and the tube was sealed; the polymerization was performed at 70 °C for 12 h. The polymerization was stopped by cooling to room temperature. The mixture was centrifuged (10 000 rev/min, 15 min) and washed five times with THF. SNT-PDEAEMA-*b*-POEGMA was dried overnight in a vacuum oven at room temperature.

2.5. pH-Dependent Release Behaviors. The loading of drug was carried out as follows. SNT-PDEAEMA-*b*-POEGMA (100 mg) and DOX (10 mg) or RhB (10 mg) and 10 mL of buffer solution (pH = 4.0) were stirred overnight at room temperature. Then the dispersion was centrifuged (10 000 r/min, 15 min) to collect the SNT-PDEAEMA-*b*-POEGMA loaded with DOX or RhB. The product was washed with aqueous solution (pH = 8.0) to remove DOX or RhB adsorbed on the surface of SNT-PDEAEMA-*b*-POEGMA. The separated supernatant solution by centrifugation and washing was collected, and the drug content loaded in SNTs was determined by fluorescence spectroscopy against the standard curve.[41] The release experiment was performed under various pHs (pH = 7.4, 5.0, and 4.0). A typical procedure was as follows. DOX-loaded SNT-PDEAEMA-*b*-POEGMA (20 mg) was stirred in various buffer solutions (50 mL, pH = 7.4, 5.0, and 4.0) at room temperature. At different time intervals, an aliquot (1 mL) was taken, and SNT-PDEAEMA-*b*-POEGMA was isolated by centrifugation. The obtained supernatant liquid was subjected to fluorescence to record the spectra to determine the amount of DOX released from SNTs.

2.6. In Vitro Cytotoxicity Assays and Endocytosis. The in vitro cytotoxicity of SNTs, SNT-PDEAEMA, and SNT-PDEAEMA-*b*-POEGMA against HepG2 cells were evaluated via MTT assay. The cells were seeded in a 96-well plates (10 000 cells/well) and incubated at 37 °C in a 5% CO_2 atmosphere with complete Dulbecco's modified Eagle's medium (DMEM) for 24 h. Then, the media in the well was replaced by fresh DMEM containing the samples with different concentrations (0−200 mg/mL). After 24 h of incubation, the culture medium was withdrawn and washed with phosphate-buffered solution (PBS) twice, and 125 μL of MTT solution (1 mg/mL) was added into each well. The culture medium was incubated further for 4 h. The medium was withdrawn, 200 μL of dimethyl sulfoxide (DMSO) was added into each well, and the plate was shaken gently. The cell viability was measured by reading the absorbance at 570 nm using a Bio-Rad

DOI: 10.1021/am507832n
ACS Appl. Mater. Interfaces 2015, 7, 3618−3625

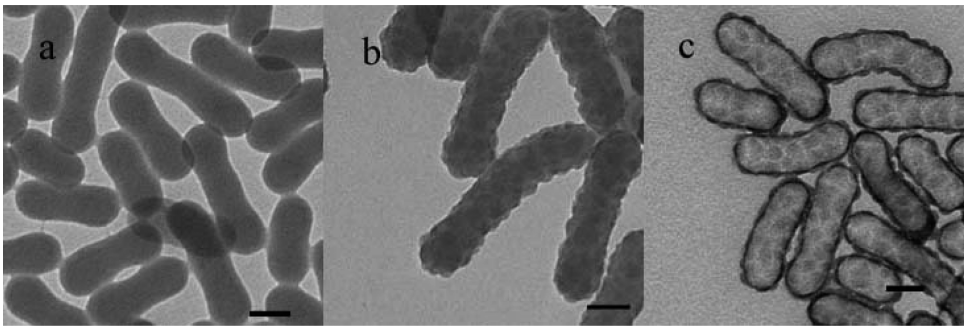

Figure 1. TEM images of polymer nanorods (a), silica/polymer hybrid nanorods (b), and silica nanotubes (c). All scale bars are 100 nm.

Scheme 1. Synthetic Route of SNT-PDEAEMA-*b*-POEGMA

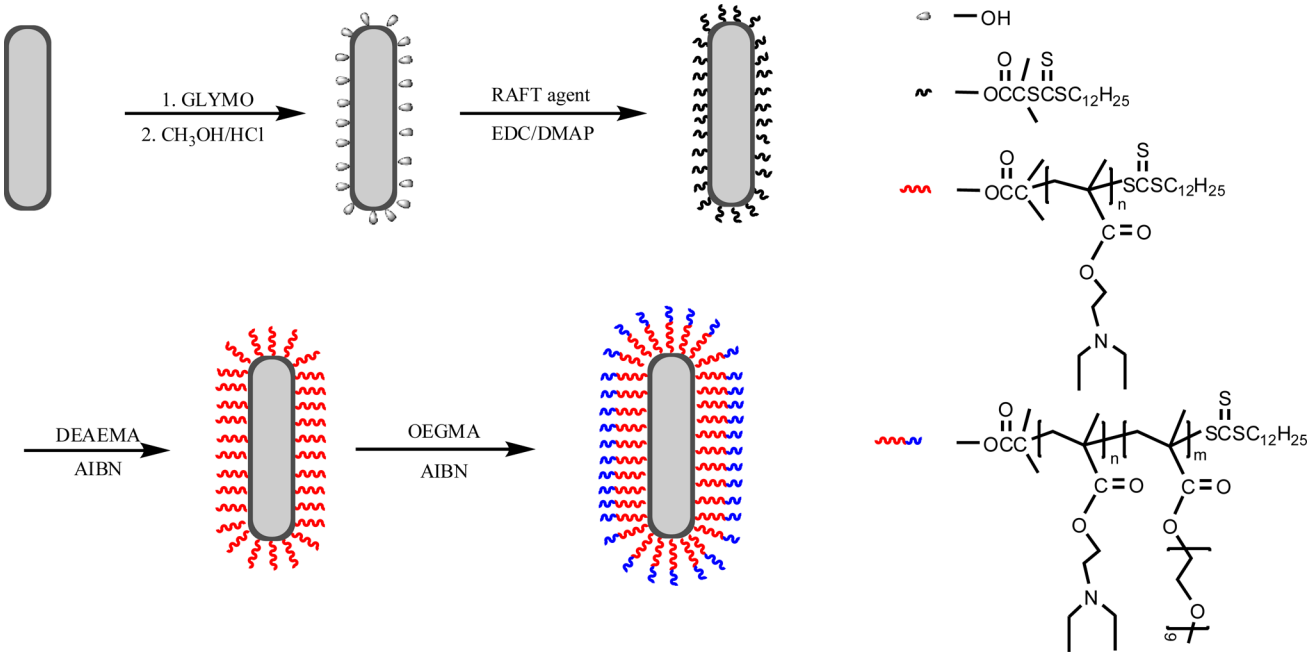

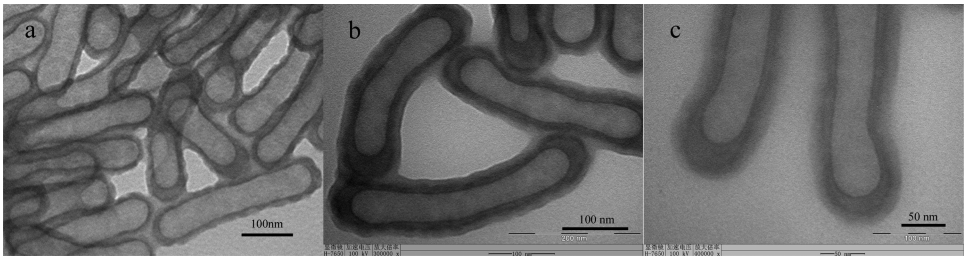

Figure 2. TEM images of SNT-PDEAEMA-*b*-POEGMA (a–c). (b, c) Magnification images.

680 microplate reader. Each experiment condition was tested in five replicates.

The cellular uptake assay of the RhB-loaded SNT-PDEAEMA-*b*-POEGMA was conducted. The HepG2 cells were seeded in a 4-well cell culture plate (40 000 cells/well) in 500 μL of DMEM medium. After incubation for 24 h at 37 °C, the culture medium in the well was replaced by DMEM with 100 μg/mL of RhB-loaded SNT-PDEAEMA-*b*-POEGMA, and cells were incubated for an additional 3 h. Subsequently, cells were washed three times with PBS. Then, the cells were visualized under a laser scanning confocal microscope.

2.7. Characterization. Nuclear magnetic resonance (NMR) spectra were recorded on a Bruker AV300 MHz spectrometer using $CDCl_3$ as solvent. Gel permeation chromatography (GPC) was performed using THF as eluent at a flow rate of 1.0 mL/min with microstyragel columns (500, 1×10^3, and 1×10^4 Å) and RI 2414 detector to determine the molecular weight (M_n) and molecular weight distribution (M_w/M_n) of the polymers. Monodispersed polystyrene standards were used to generate the calibration curve. The morphologies of samples were recorded on a Hitachi 7650 transmission electron microscope (TEM) operating at 100 kV. To prepare the TEM sample, nanoparticle was dispersed in ethanol, and one drop of the dispersion was deposited onto a copper grid and dried naturally before characterization. Nitrogen adsorption/desorption analysis was conducted at 77 K on an ASAP 2020 micromeritics porosimeter. Fourier transform infrared (FT-IR) measurements were performed on a Bruker VECTOR-22 IR spectrometer. Thermal gravimetric analyses (TGA) were conducted on PerkinElmer Diamond TG/DTA Instruments with a nitrogen flow, and the heating rate was

DOI: 10.1021/am507832n
ACS Appl. Mater. Interfaces 2015, 7, 3618–3625

10 °C/min. Fluorescence spectra were recorded on a RF-5301PC fluorescence spectrometer. Confocal laser scanning microscopic images were recorded on a Leica Microsystems fluorescence microscopy.

3. RESULTS AND DISCUSSION

3.1. Preparation and Characterization of Silica Nanotubes. Polymer nanorods were used as templates to fabricate the SNTs. According to our previous work,[36] polymer nanorods were prepared via PISR method, and the polymerization procedure is shown in Supporting Information, Scheme S1. First, CPDB-terminated PDMAEMA was synthesized and purified, and ^{1}H NMR spectroscopy and GPC analyses were used to characterize PDMAEMA. The mean degree of polymerization (DP) of PDMAEMA was determined to be 149 based on the integral values of the peaks at 4.07 and 7.2–8.0 ppm (Supporting Information, Figure S1A). The GPC curve (Supporting Information, Figure S2A) indicated a narrow polydispersity of 1.11. RAFT polymerization of styrene was then carried out in methanol, where CPDB-terminated PDMAEMA was used as macro RAFT agent and stabilizer. Polymer nanorods composed of diblock copolymer PDMAEMA-*b*-PS were obtained. The ^{1}H NMR spectrum of PDMAEMA-*b*-PS is shown in Supporting Information, Figure S1B. All characteristic peaks were marked clearly, and the DP of PS block was calculated to be 2505 based on the integral values of the signals at 6.2–7.2 and 4.07 ppm. The GPC curve of PDMAEMA-*b*-PS (Supporting Information, Figure S2B) indicates a polydispersity of 1.22. TEM image of polymer nanorods is shown in Figure 1a. The lengths of polymer nanorods range from 200 to 400 nm, and the average diameter of nanorods is 93 nm.

TEOS was used as the silica precursor, and deposition of silica onto the polymer nanorods was performed in a solution of HCl in methanol–water (1/1, v/v) at room temperature. The weak polyelectrolyte PDMAEMA containing tertiary

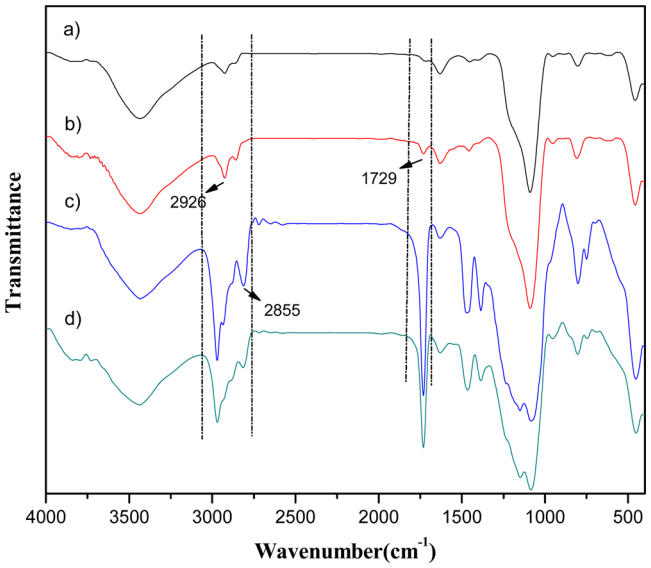

Figure 3. FT-IR spectra of SNT–OH (a), SNT-RAFT (b), SNT-PDEAEMA (c), and SNT-PDEAEMA-*b*-POEGMA (d).

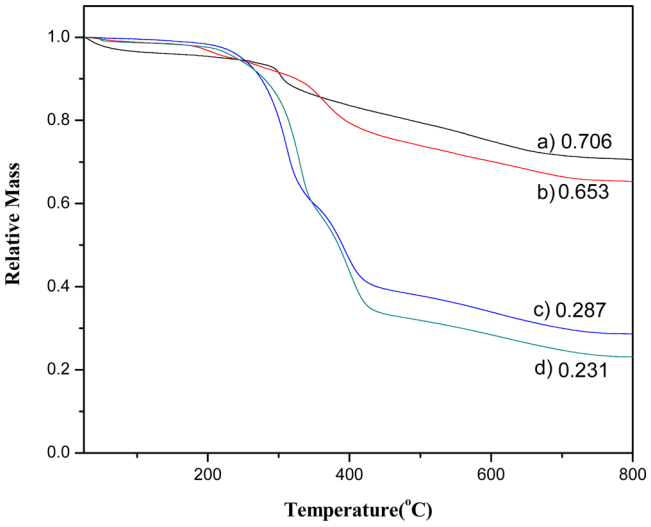

Figure 4. TGA curves of SNT-OH (a), SNT-RAFT (b), SNT-PDEAEMA (c), and SNT-PDEAEMA-*b*-POEGMA (d).

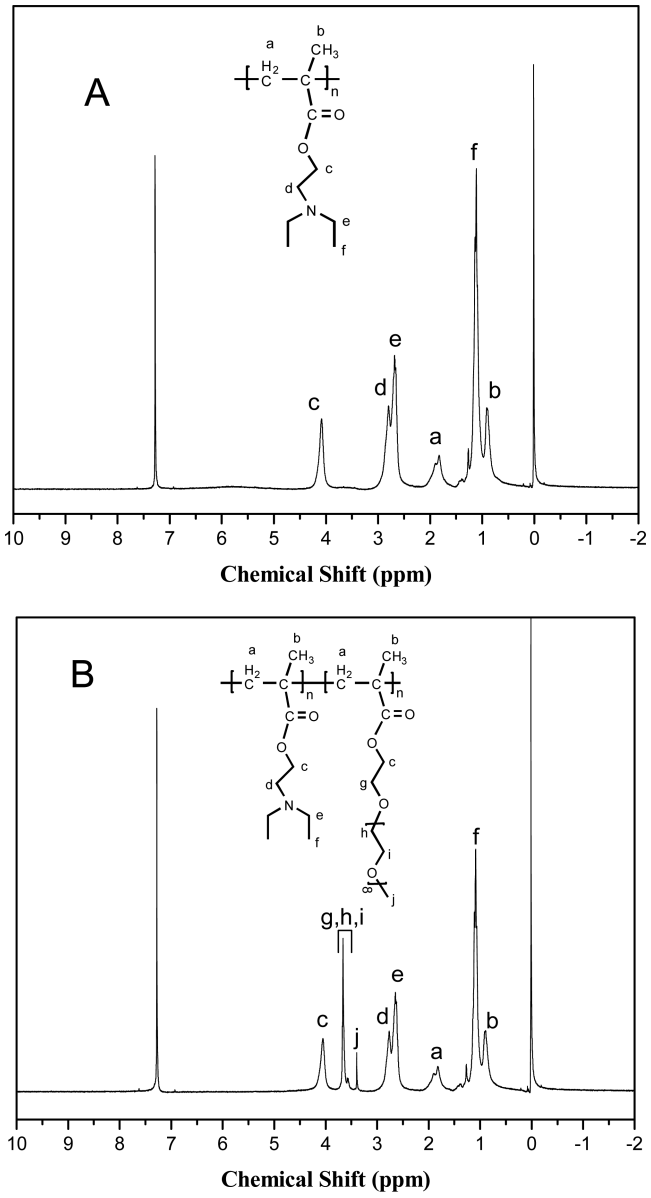

Figure 5. ^{1}H NMR spectra of PDEAEMA (A) and PDEAEMA-*b*-POEGMA (B) cleaved from SNT-PDEAEMA and SNT-PDEAEMA-*b*-POEGMA in $CDCl_3$, respectively.

DOI: 10.1021/am507832n
ACS Appl. Mater. Interfaces 2015, 7, 3618–3625

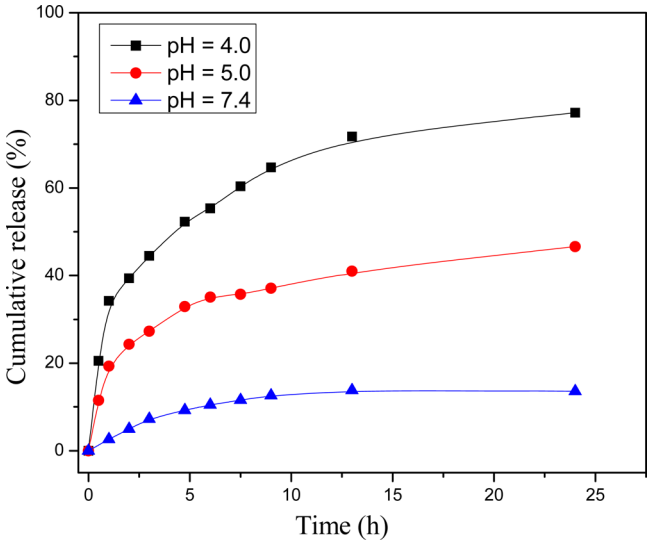

Figure 6. Time evolution of DOX release from SNT-PDEAEMA-*b*-POEGMA at different pH values.

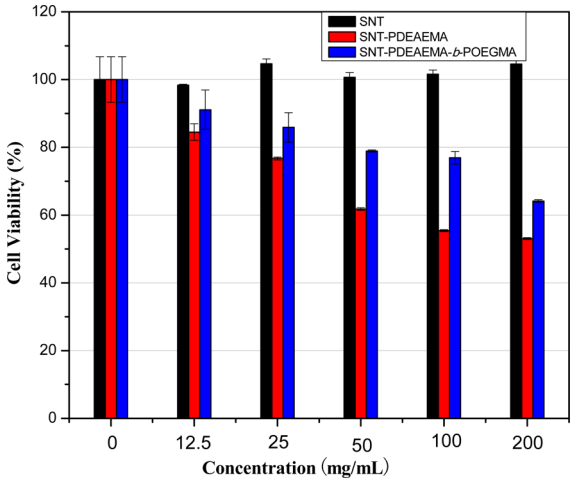

Figure 7. In vitro cell viability of HepG2 cells incubated with various concentrations of SNTs, SNT-PDEAEMA, and SNT-PDEAEMA-*b*-POEGMA determined by MTT assay in 24 h.

amine groups, as the nanoreactor for deposition of silica, could catalyze the hydrolysis and polycondensation of TEOS. Hydrolyzed TEOS precursors migrated into the protonated ammonium sites in PDMAEMA via charge driving and underwent condensation in the shell of polymer nanorods, which resulted in silica/polymer hybrid nanorods.[31]

TEM image of silica/polymer hybrid nanorods is shown in Figure 1b. The surfaces of silica/polymer hybrids (Figure 1b) are coarser compared with the smooth surfaces of polymer nanorods (Figure 1a). The length range of hybrid nanorods is similar to that of the corresponding polymer nanorods, and the average diameter of the hybrid nanorods is 108 nm. After calcination of hybrid nanorods at 550 °C for 5 h, the polymers were completely removed, and SNTs were obtained. As shown in Figure 1c, SNTs possess hollow structure, and both sides of them are closed. The average diameter and wall thickness of the SNTs are 95 and 16 nm, respectively.

During the deposition process of silica onto the surface of templates, the PDMAEMA chains were enveloped within the silica shell, and removal of these chains generated micropores. A typical hysteresis loop is shown in the nitrogen adsorption/desorption analysis of SNTs (Supporting Information, Figure S3), indicating micropores exist in SNTs. The BJH pore-size distribution curve (inset picture) indicates that the peak value of pore size is ∼1.4 nm. The Brunauer−Emmett−Teller surface is 164.5 m^2/g and the micropore area and micropore volume are 114.2 m^2/g and 0.059 cm^3/g, respectively. The hollow SNTs are accessible to small molecules through the micropores; thus, SNTs are expected to be used as drug vehicle.

3.2. Preparation and Characterization of SNT-PDEAEMA-*b*-POEGMA. The synthetic route of SNT-PDEAEMA-*b*-POEGMA is shown in Scheme 1. To graft PDEAEMA-*b*-POEGMA onto the surface of SNTs, RAFT agent must be anchored on the surface of SNTs. First, GLYMO reacted with the silanol of SNTs, introducing epoxy groups onto the exterior surface of SNTs and forming GLYMO-coated SNTs. After converting epoxy groups to hydroxyl groups in methanol, RAFT agent functionalized SNTs (SNT-RAFT) were obtained by esterification reaction of *S*-1-dodecyl-*S*′-(α,α′-dimethyl-α″-acetic acid) trithiocarbonate with hydroxyl groups under the catalysis of EDC and DMAP. Subsequently, PDEAEMA chains were grafted onto the exterior surface of SNTs via RAFT polymerization using SNT-RAFT as RAFT agent. SNT-PDEAEMA-*b*-POEGMA was then synthesized using SNT-PDEAEMA as RAFT agent in the surface RAFT polymerization of OEGMA.

Figure 2 shows the TEM images of SNT-PDEAEMA-*b*-POEGMA. In contrast to bare SNTs (Figure 1c), an apparent polymer layer around the exterior surface of SNTs certifies that polymers are successfully grafted onto the exterior surface of SNTs through RAFT polymerization. The average thickness of

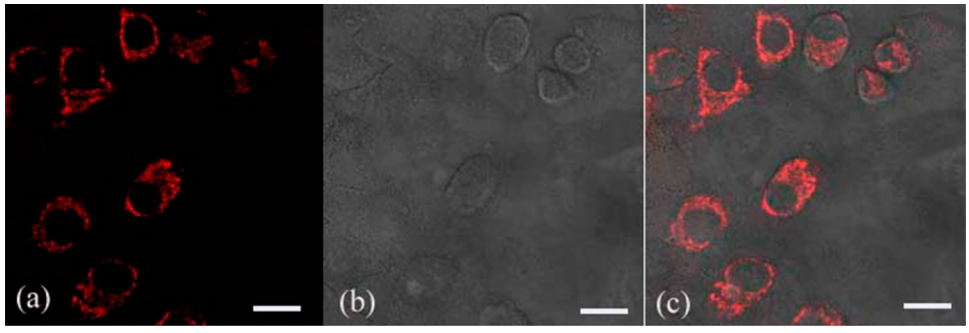

Figure 8. CLSM images of cellular uptake of RhB-loaded SNT-PDEAEMA-*b*-POEGMA (100 μg/mL) after incubation with HepG2 cells under (a) excitation at λ_{ex} = 520 nm, (b) bright field, and (c) merged image of (a) and (b). The scale bars are 20 μm.

DOI: 10.1021/am507832n
ACS Appl. Mater. Interfaces 2015, 7, 3618−3625

polymer shell is ~10 nm according to the TEM image. FT-IR spectra of SNT-OH, SNT-RAFT, SNT-PDEAEMA, and SNT-PDEAEMA-*b*-POEGMA are shown in Figure 3. The comparison of the FT-IR spectrum for SNT-OH (Figure 3a) and SNT-RAFT (Figure 3b) shows that a new absorption band at 1729 cm^{-1} appears in Figure 3b, which is characteristic absorption peak of C═O in ester groups, providing evidence of the successful grafting of RAFT agent. Meanwhile, a slight strengthening of absorption peaks at 1465, 2926, and 2855 cm^{-1} compared to those of SNT-OH can be observed, which is ascribed to the C−H vibrations of RAFT agents in SNT-RAFT. In the FT-IR spectrum of SNT-PDEAEMA (Figure 3c), absorption bands at 1729, 2926, 2855, and 1465 cm^{-1} increase significantly due to the introduction of a large number of C═O and C−H groups. Besides, there is no obvious difference between the FT-IR spectra of SNT-PDEAEMA (Figure 3c) and SNT-PDEAEMA-*b*-POEGMA (Figure 3d), because no new characteristic group appears.

The TGA curves of SNT-OH, SNT-RAFT, SNT-PDEAEMA, and SNT-PDEAEMA-*b*-POEGMA are shown in Figure 4. The weight losses of SNT-OH (Figure 4a) and SNT-RAFT (Figure 4b) are 29.4% and 34.7%, respectively. The grafting content of RAFT agents is 0.32 mmol/g of SiO_2. The weight losses of SNT-PDEAEMA and SNT-PDEAEMA-*b*-POEGMA are 71.3% and 76.9%, respectively, indicating that PDEAEMA and PDEAEMA-*b*-POEGMA are successfully grafted on the surface of SNTs.

PDEAEMA and PDEAEMA-*b*-POEGMA were cleaved from polymer-coated SNTs by HF solution,[42] and the retrieved polymers were characterized by ^{1}H NMR analysis. In the ^{1}H NMR spectrum of PDEAEMA (Figure 5A), the signals at δ = 1.6−2.1 (a) and 0.9 ppm (b) are attributed to the protons of methylene and methyl groups in main chain, respectively. The peak of ester methylene protons appears at 4.05 ppm (c). The signals at δ = 2.82 (d), 2.67 (e), and 1.09 ppm (f) are assigned to the methylene protons adjacent to the diethylamino group, the methylene protons of diethylamino group, and the methyl protons of diethylamino group, respectively. The ^{1}H NMR spectrum of PDEAEMA-*b*-POEGMA (Figure 5B) reveals signals of both PDEAEMA and POEGMA. The characteristic peaks of POEGMA appearing at δ = 3.4 (j) and 3.5−3.8 ppm (g−i) are ascribed to ether methoxy and methylene protons in the side chains. The molar ratio of DEAEMA to OEGMA units in PDEAEMA-*b*-POEGMA is ~12:1, which is calculated from the integral values of the peaks at δ = 4.05 ppm (c) and δ = 3.4 ppm (j).

3.3. pH-Dependent Release Behavior of SNT-PDEAEMA-*b*-POEGMA. To study pH-dependent release behavior of SNT-PDEAEMA-*b*-POEGMA as vehicle, DOX was loaded in SNT-PDEAEMA-*b*-POEGMA. SNT-PDEAEMA-*b*-POEGMA was dispersed in aqueous solution (pH = 4.0) of DOX, and the mixture was stirred overnight. The DOX-loaded SNT-PDEAEMA-*b*-POEGMA was isolated by centrifugation and washed by alkaline water adequately to remove the unloaded DOX. Subsequently, the release study was conducted under various pHs. The three aliquots of SNT-PDEAEMA-*b*-POEGMA loaded with DOX were placed in buffer solutions at different pH (pH = 7.4, 5.0, 4.0) with sufficient stirring. At the predetermined time interval, an aliquot (1 mL) was taken,SNT-PDEAEMA-*b*-POEGMA was isolated by centrifugation, and the obtained supernatant liquid was subjected to fluorescence to record the spectra. The released percentage of DOX was calculated based on the standard curves of fluorescent intensity versus concentration of DOX at different pH. The pH-dependent release profiles of encapsulated DOX from SNT-PDEAEMA-*b*-POEGMA are shown in Figure 6. Approximately 13% DOX was released from DOX-loaded SNT-PDEAEMA-*b*-POEGMA at pH 7.4 within 24 h. A relatively low released percentage of DOX is observed, which is because the PDEAEMA chains grafted on SNTs are collapsed and block the diffusion of DOX from the inside of SNTs. By comparison, the release amount of DOX is 77% after 24 h at pH 4.0, much higher than that at pH 7.4. This is mainly due to the PDEAEMA chains being protonated and stretched in the open state, which is beneficial to the release of DOX. When the release was conducted at pH = 5.0, the released percentage of RhB after 24 h is 47%, which is less than that at pH = 4.0. This is understandable by considering that PDEAEMA chains are not protonated completely when the pH increased to 5.0, and the less stretched PDEAEMA chains would delay the release of guest molecules from SNT-PDEAEMA-*b*-POEGMA to some extent. The release experiment demonstrates the controlled release of DOX from this pH-responsive nanocarrier by adjusting pH of the medium.

3.4. In Vitro Cell Viability and Cell Uptake Properties. The cytotoxicity of SNTs, SNT-PDEAEMA, and SNT-PDEAEMA-*b*-POEGMA was evaluated by MTT assay using HepG2 cells (Figure 7). SNTs showed no obvious toxicity on cells at 200 μg/mL after 24 h of incubation. SNT-PDEAEMA-*b*-POEGMA was less toxic than SNT-PDEAEMA, which is because the biocompatible POEGMA located in the outside layer of the polymer shell can reduce the toxicity of SNT-PDEAEMA-*b*-POEGMA. Considering that the cell viability for SNT-PDEAEMA-*b*-POEGMA was nearly 80% at concentration of 100 μg/mL after 24 h of incubation, this SNT-PDEAEMA-*b*-POEGMA has relatively low cytotoxicity and is suitable for further biological applications.

Confocal laser scanning microscopic (CLSM) was used to investigate the cellular uptake property of SNT-PDEAEMA-*b*-POEGMA. Before characterization, HepG2 cells were incubated in DMEM with RhB-loaded SNT-PDEAEMA-*b*-POEGMA for 3 h at 37 °C. In the resultant images (Figure 8), red fluorescence was observed in HepG2 cells, revealing that RhB-loaded SNT-PDEAEMA-*b*-POEGMA could be endocytosed by cells successfully. Since there was no obvious fluorescence observed in the nucleus, RhB-loaded SNT-PDEAEMA-*b*-POEGMA was located in the cytoplasm of cells.

4. CONCLUSIONS

A novel drug carrier based on SNTs functionalized by pH-responsive diblock copolymer PDEAEMA-*b*-POEGMA has been successfully prepared. PISR method was used to prepare polymer nanorods as template to fabricate SNTs conveniently, and the diblock copolymers PDEAEMA-*b*-POEGMA were grafted to SNTs via surface RAFT polymerization. The SNTs show well-defined structure, and micropores existing in the walls provide channels for small molecules passing into SNTs. Because of the pH-responsiveness of polymer grafted on SNTs, the controlled release of DOX molecules from SNT-PDEAEMA-*b*-POEGMA can be achieved by adjusting the pH of medium. The results of in vitro cell viability and cellular internalization study indicate that PDEAEMA-*b*-POEGMA-coated SNTs have good biocompatibility and excellent endocytosis property. We vision that this drug carrier will contribute to the expansion of the variety of vehicles and may be applied to drug and gene delivery.

DOI: 10.1021/am507832n
ACS Appl. Mater. Interfaces 2015, 7, 3618−3625

■ ASSOCIATED CONTENT

Supporting Information

The synthesis procedure of polymer nanorods; ^{1}H NMR spectra and GPC traces of PDMAEMA and PDMAEMA-*b*-PS; adsorption/desorption isotherms for SNTs; BJH pore-size distribution plot of SNTs. This material is available free of charge via the Internet at http://pubs.acs.org.

■ AUTHOR INFORMATION

Corresponding Author

*E-mail: hongcy@ustc.edu.cn.

Notes

The authors declare no competing financial interest.

■ ACKNOWLEDGMENTS

This research was supported by National Natural Science Foundation of China (Nos. 21374107 and 21090354) and the Fundamental Research Funds for the Central Universities (WK 2060200012).

■ REFERENCES

(1) Malmsten, M. Soft Drug Delivery Systems. *Soft Matter* **2006**, *2*, 760−769.
(2) Kedar, U.; Phutane, P.; Shidhaye, S.; Kadam, V. Advances in Polymeric Micelles for Drug Delivery and Tumor Targeting. *Nanomedicine* **2010**, *6*, 714−729.
(3) Kabanov, A. V. Polymer Genomics: An Insight into Pharmacology and Toxicology of Nanomedicines. *Adv. Drug Delivery Rev.* **2006**, *58*, 1597−1621.
(4) Bysell, H.; Mansson, R.; Hansson, P.; Malmsten, M. Microgels and Microcapsules in Peptide and Protein Drug Delivery. *Adv. Drug Delivery Rev.* **2011**, *63*, 1172−1185.
(5) Liu, T.; Zhang, Y. F.; Liu, S. Y. Drug and Plasmid DNA co-Delivery Nanocarriers Based on ABC-type Polypeptide Hybrid Miktoarm Star Copolymers. *Chin. J. Polym. Sci.* **2013**, *31*, 924−937.
(6) Malmsten, M. Inorganic Nanomaterials as Delivery Systems for Proteins, Peptides, DNA, and SiRNA. *Curr. Opin. Colloid Interface Sci.* **2013**, *18*, 468−480.
(7) Singh, R. K.; Kim, H. W. Inorganic Nanobiomaterial Drug Carriers for Medicine. *Tissue Eng. Regener. Med.* **2013**, *10*, 296−309.
(8) Slowing, I. I.; Vivero-Escoto, J. L.; Wu, C. W.; Lin, V. S.-Y. Mesoporous Silica Nanoparticles as Controlled Release Drug Delivery and Gene Transfection Carriers. *Adv. Drug Delivery Rev.* **2008**, *60*, 1278−1288.
(9) Slowing, I. I.; Trewyn, B. G.; Giri, S.; Lin, V. S. Y. Mesoporous Silica Nanoparticles for Drug Delivery and Biosensing Applications. *Adv. Funct. Mater.* **2007**, *17*, 1225−1236.
(10) Vivero-Escoto, J. L.; Slowing, I. I.; Trewyn, B. G.; Lin, V. S. Y. Mesoporous Silica Nanoparticles for Intracellular Controlled Drug Delivery. *Small* **2010**, *6*, 1952−1967.
(11) Tang, F.; Li, L.; Chen, D. Mesoporous Silica Nanoparticles: Synthesis, Biocompatibility and Drug Delivery. *Adv. Mater.* **2012**, *24*, 1504−1534.
(12) Qiao, Z. A.; Huo, Q. S.; Chi, M. F.; Veith, G. M.; Binder, A. J.; Dai, S. A "Ship-In-A-Bottle" Approach to Synthesis of Polymer Dots@Silica or Polymer Dots@Carbon Core-Shell Nanospheres. *Adv. Mater.* **2012**, *24*, 6017−6021.
(13) Müller, M.; Lunkenbein, T.; Breu, J.; Caruso, F.; Müller, A. H. E. Template-Directed Synthesis of Silica Nanowires and Nanotubes from Cylindrical Core-Shell Polymer Brushes. *Chem. Mater.* **2012**, *24*, 1802−1810.
(14) Yuan, J. Y.; Xu, Y. Y.; Walther, A.; Bolisetty, S.; Schumacher, M.; Schmalz, H.; Ballauff, M.; Müller, A. H. E. Water-Soluble Organo-Silica Hybrid Nanowires. *Nat. Mater.* **2008**, *7*, 718−722.
(15) Sun, J. T.; Piao, J. G.; Wang, L. H.; Javed, M.; Hong, C. Y.; Pan, C. Y. One-Pot Synthesis of Redox-Responsive Polymers-Coated Mesoporous Silica Nanoparticles and Their Controlled Drug Release. *Macromol. Rapid Commun.* **2013**, *34*, 1387−1394.
(16) Mal, N. K.; Fujiwara, M.; Tanaka, Y. Photocontrolled Reversible Release of Guest Molecules from Coumarin-Modified Mesoporous Silica. *Nature* **2003**, *421*, 350−353.
(17) Vivero-Escoto, J. L.; Slowing, I. I.; Wu, C. W.; Lin, V. S.-Y. Photoinduced Intracellular Controlled Release Drug Delivery in Human Cells by Gold-Capped Mesoporous Silica Nanosphere. *J. Am. Chem. Soc.* **2009**, *131*, 3462−3463.
(18) Arcos, D.; Vallet-Regi, M. Bioceramics for Drug Delivery. *Acta Mater.* **2013**, *61*, 890−911.
(19) Wan, X.; Wang, D.; Liu, S. Fluorescent pH-Sensing Organic/Inorganic Hybrid Mesoporous Silica Nanoparticles with Tunable Redox-Responsive Release Capability. *Langmuir* **2010**, *26*, 15574−15579.
(20) Huang, X. L.; li, L. L.; Liu, T. L.; Hao, N. J.; Liu, H. Y.; Chen, D.; Tang, F. Q. The Shape Effect of Mesoporous Silica Nanoparticles on Biodistribution, Clearance, and Biocompatibility in Vivo. *ACS Nano* **2011**, *5*, 5390−5399.
(21) Huang, X. L.; Teng, X.; Chen, D.; Tang, F. Q.; He, J. Q. The Effect of the Shape of Mesoporous Silica Nanoparticles on Cellular Uptake and Cell Function. *Biomaterials* **2010**, *31*, 438−448.
(22) Yang, Y.; Suzuki, M.; Owa, S.; Shirai, H.; Hanabusa, K. J. Control of Helical Silica Nanostructures Using a Chiral Surfactant. *J. Mater. Chem.* **2006**, *16*, 1644−1650.
(23) Zhang, Z.; Buitenhuis, J. Synthesis of Uniform Silica Rods, Curved Silica Wires, and Silica Bundles Using Filamentous fd Virus as a Template. *Small* **2007**, *3*, 424−428.
(24) Gao, C.; Lu, Z.; Yin, Y. Gram-Scale Synthesis of Silica Nanotubes with Controlled Aspect Ratios by Templating of Nickel-Hydrazine Complex Nanorods. *Langmuir* **2011**, *27*, 12201−12208.
(25) Kim, F. S.; Ren, G. Q.; Jenekhe, S. A. One-Dimensional Nanostructures of π-Conjugated Molecular Systems: Assembly, Properties, and Applications from Photovoltaics, Sensors, and Nanophotonics to Nanoelectronics. *Chem. Mater.* **2011**, *23*, 682−732.
(26) Yuan, J. Y.; Xu, Y. Y.; Müller, A. H. E. One-Dimensional Magnetic Inorganic−Organic Hybrid Nanomaterials. *Chem. Soc. Rev.* **2011**, *40*, 640−655.
(27) Müllner, M.; Yuan, J. Y.; Weiss, S.; Walther, A.; Fortsch, M.; Drechsler, M.; Müller, A. H. E. Water-Soluble Organo-Silica Hybrid Nanotubes Templated by Cylindrical Polymer Brushes. *J. Am. Chem. Soc.* **2010**, *132*, 16587−16592.
(28) Zheng, Z. C.; Daniel, A.; Yu, W.; Weber, B.; Ling, J.; Müller, A. H. E. Rare-Earth Metal Cations Incorporated Silica Hybrid Nanoparticles Templated by Cylindrical Polymer Brushes. *Chem. Mater.* **2013**, *25*, 4585−4594.
(29) Wang, H.; Patil, A. J.; Liu, K.; Petrov, S.; Mann, S.; Winnik, M. A.; Manners, I. Fabrication of Continuous and Segmented Polymer/Metal Oxide Nanowires Using Cylindrical Micelles and Block Comicelles as Templates. *Adv. Mater.* **2009**, *21*, 1805−1808.
(30) Zhang, M. C.; Zhang, W. Q.; Wang, S. N. Synthesis of Well-Defined Silica and Pd/Silica Nanotubes through a Surface Sol-Gel Process on a Self-Assembled Chelate Block Copolymer. *J. Phys. Chem. C* **2010**, *114*, 15640−15644.
(31) Yang, L. P.; Zou, P.; Pan, C. Y. Preparation of Hierarchical Worm-Like Silica Nanotubes. *J. Mater. Chem.* **2009**, *19*, 1843−1849.
(32) Yuwono, V. M.; Hartgerink, J. D. Peptide Amphiphile Nanofibers Template and Catalyze Silica Nanotube Formation. *Langmuir* **2007**, *23*, 5033−5038.
(33) Wan, W. M.; Sun, X. L.; Pan, C. Y. Formation of Vesicular Morphologies via Polymerization Induced Self-Assembly and Re-Organization. *Macromol. Rapid Commun.* **2010**, *31*, 399−404.
(34) Wan, W. M.; Hong, C. Y.; Pan, C. Y. One-Pot Synthesis of Nanomaterials via RAFT Polymerization Induced Self-Assembly and Morphology Transition. *Chem. Commun.* **2009**, 5883−5995.
(35) Cai, W. M.; Wan, W. M.; Hong, C. Y.; Huang, C. Q.; Pan, C. Y. Morphology Transitions in RAFT Polymerization. *Soft Matter* **2010**, *6*, 5554−5561.

DOI: 10.1021/am507832n
ACS Appl. Mater. Interfaces 2015, 7, 3618−3625

(36) Zhang, W. J.; Hong, C. Y.; Pan, C. Y. Fabrication and Characterization of Silica Nanotubes with Controlled Dimensions. *J. Mater. Chem. A* **2014**, *2*, 7819−7828.
(37) Engin, K.; Leeper, D. B.; Cater, J. R.; Thistlethwaite, A. J.; Tupchong, L.; Mcfarlane, J. D. Extracellular pH Distribution in Human Tumors. *Int. J. Hypertherm.* **1995**, *11*, 211−216.
(38) Ma, H. W.; Hyun, J. H.; Stiller, P.; Chilkoti, A. "Non-fouling" Oligo(ethylene glycol)-Functionalized Polymer Brushes Synthesized by Surface-Initiated Atom Transfer Radical Polymerization. *Adv. Mater.* **2004**, *16*, 338−341.
(39) Mitsukami, Y.; Donovan, M. S.; Lowe, A. B.; McCormick, C. L. Water-Soluble Polymers. 81. Direct Synthesis of Hydrophilic Styrenic-Based Homopolymers and Block Copolymers in Aqueous Solution via RAFT. *Macromolecules* **2001**, *34*, 2248−2256.
(40) Lai, J. T.; Filla, D.; Shea, R. Functional Polymers from Novel Carboxyl-Terminated Trithiocarbonates as Highly Efficient RAFT Agents. *Macromolecules* **2002**, *35*, 6754−6756.
(41) Sun, J. T.; Yu, Z. Q.; Hong, C. Y.; Pan, C. Y. Biocompatible Zwitterionic Sulfobetaine Copolymer-Coated Mesoporous Silica Nanoparticles for Temperature-Responsive Drug Release. *Macromol. Rapid Commun.* **2012**, *33*, 811−818.
(42) Sun, J. T.; Hong, C. Y.; Pan, C. Y. Fabrication of PDEAEMA-Coated Mesoporous Silica Nanoparticles and pH-Responsive Controlled Release. *J. Phys. Chem. C* **2010**, *114*, 12481−12486.

DOI: 10.1021/am507832n
ACS Appl. Mater. Interfaces 2015, 7, 3618−3625